Degradation of GFRP-plates bonded to concrete: An experimental approach based on Mohr-Coulomb failure criterion

Data · June 2011

CITATIONS
0

READS
45

3 authors:

Hugo Biscaia
New University of Lisbon
98 PUBLICATIONS **575** CITATIONS
SEE PROFILE

Manuel A G Silva
New University of Lisbon
136 PUBLICATIONS **1,072** CITATIONS
SEE PROFILE

Carlos Chastre
New University of Lisbon
130 PUBLICATIONS **759** CITATIONS
SEE PROFILE

FACULDADE DE CIÊNCIAS E TECNOLOGIA
UNIVERSIDADE NOVA DE LISBOA

Degradation of GFRP-plates bonded to concrete: An experimental approach based on Mohr-Coulomb failure criterion

Hugo Biscaia, Manuel Gonçalves da Silva & Carlos Chastre

Faculdade de Ciências e Tecnologia, Universidade Nova de Lisboa, Portugal

Objectives of the study

An experimental programme was conducted in order to:

1. Characterize the glass FRP/concrete interface by double shear tests;

2. Analyse the degradation imposed to the GFRP/concrete interface by humidity salted environments;

3. The lack of information about the modelling of the interface between FRPs and concrete is a very actual theme and this work is a contribution to mitigate this gap. However, at this point of the study only reference specimens were modulated, i.e., without ageing.

4. Make proposals in order to adjust some rules or national codes.

Accelerated ageing tests

Wet and dry cycles with 5% of salt

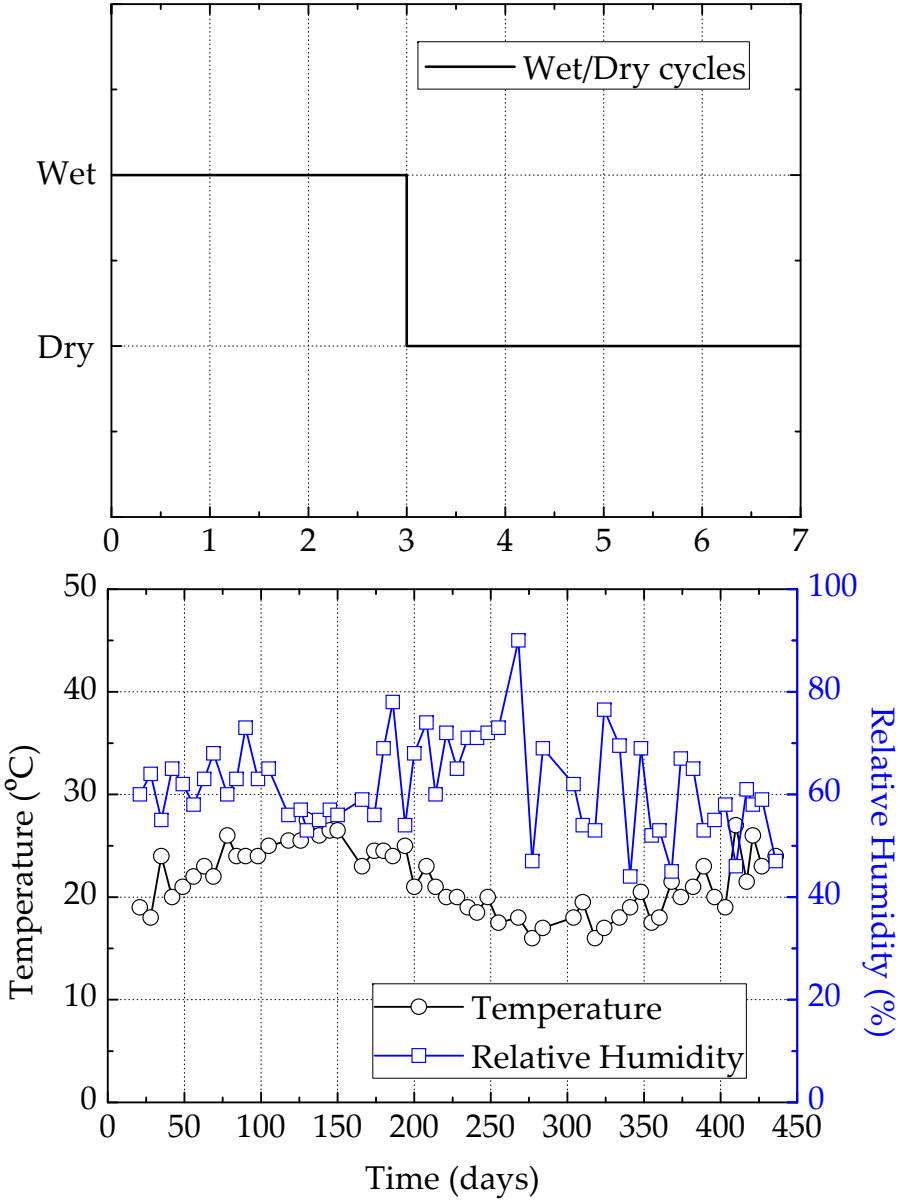

Accelerated ageing tests

Salt fog cycles (5% of salt)

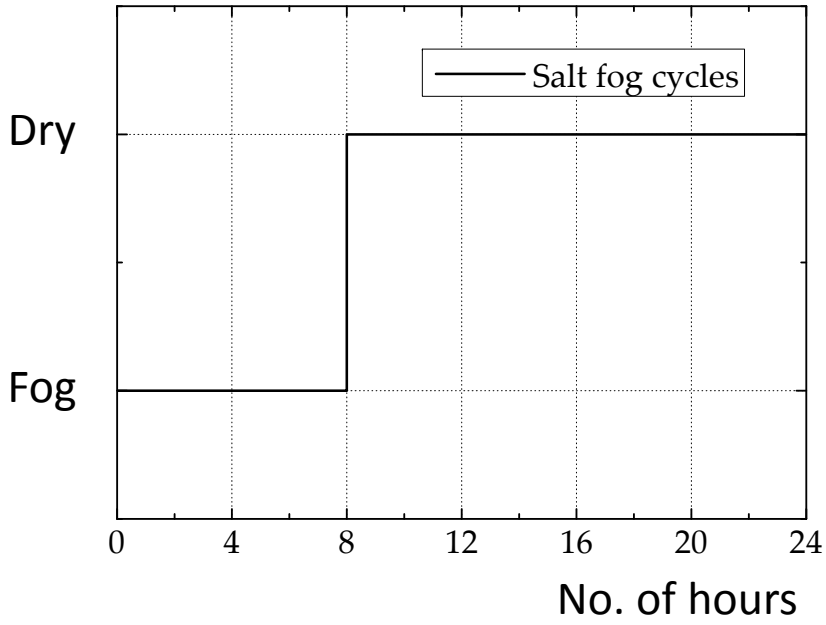

Surface treatment

Dry sand blasting with 4 bar of pressure.

Proposed shear tests

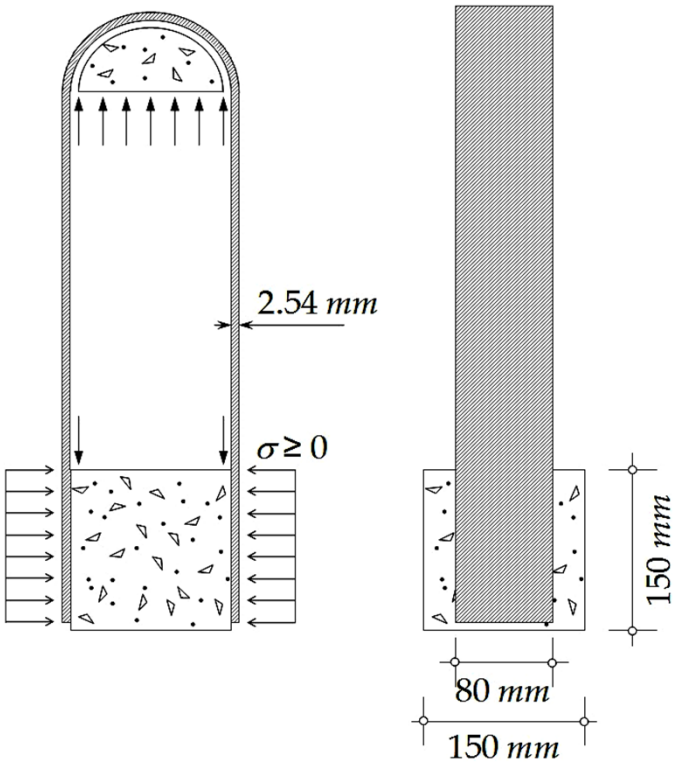

Characterization of materials

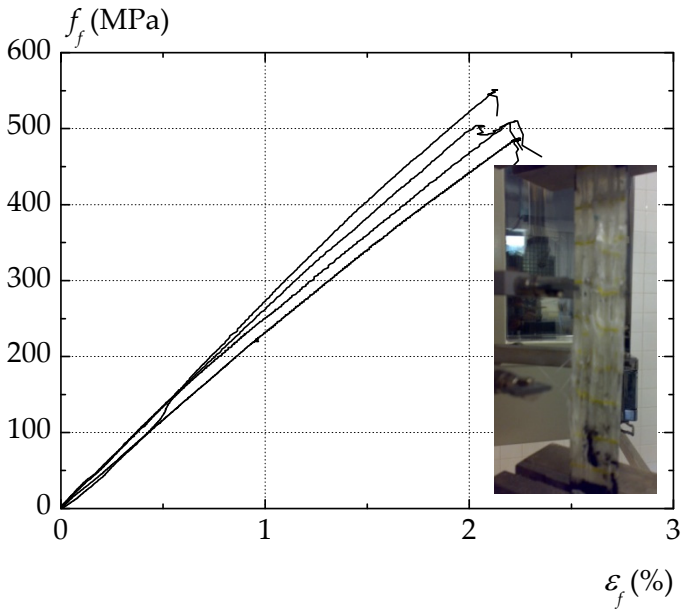

Tensile strength of the GFRP flat coupons

Concrete strength

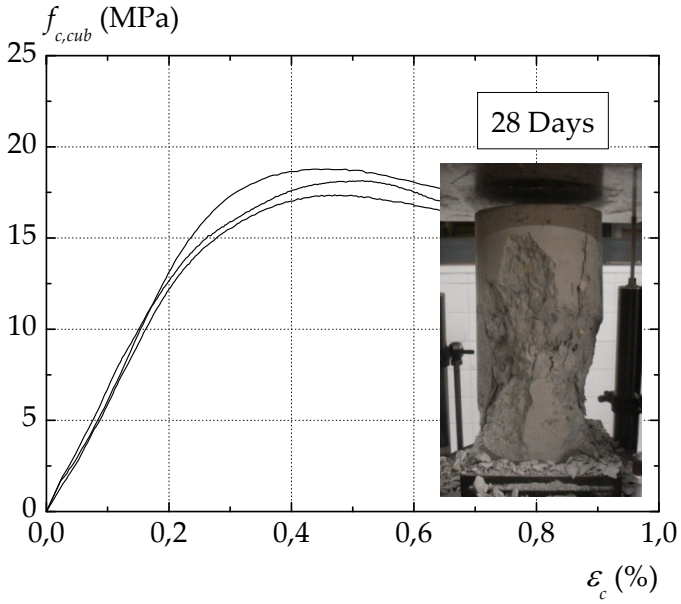

GFRP properties:

Flat coupons	ε_{fm} (%)	f_{fm} (MPa)	E_{fm} (MPa)
Reference	2.20	513.9	23.49

Concrete properties:

$f_{cm,cub}$ (MPa)	f_{cm} (MPa)	f_{ctm} (*) (MPa)	ε_{c1} (*) (%)	$f_{ctm,sp}$ (*) (MPa)	E_{cm} (*) (GPa)
18.6	16.9	1.65	0.17	1.83	23.18

(*) According to EC2.

Experimental tests

Reference specimens (at 0h of exposure)

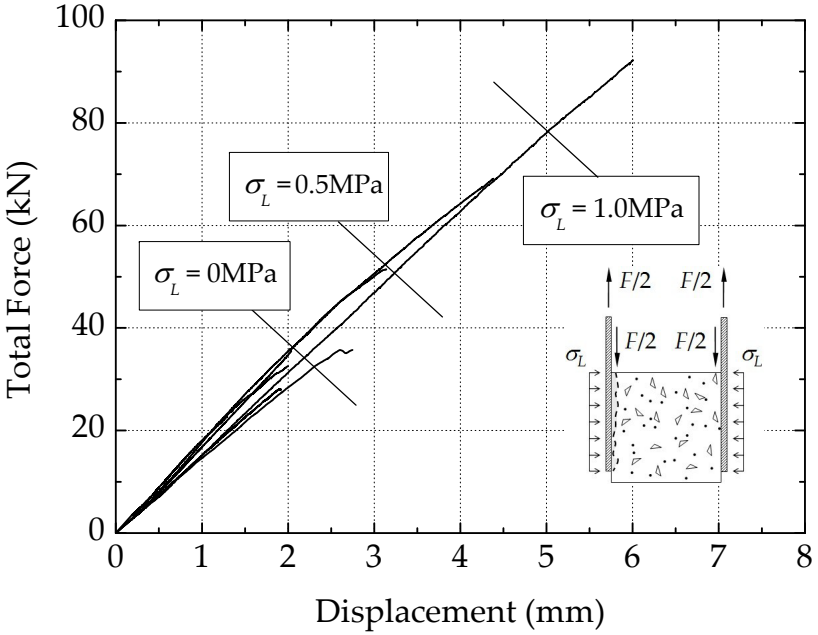

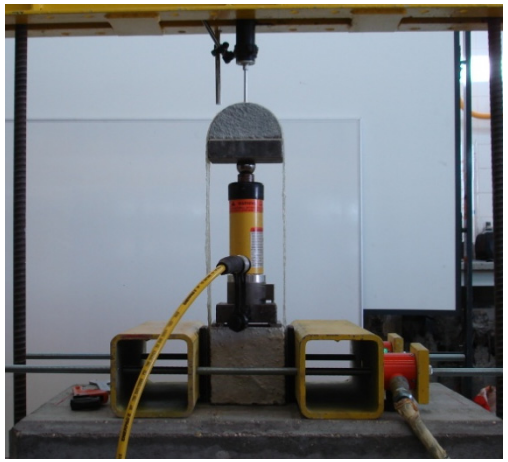

Specimen	F_{max} (kN)	Média	δ_{max} (mm)	Média
MC-REF80-01	17.86		2.60	
MC-REF80-02	16.28	16.06	2.10	2.20
MC-REF80-02a	14.03		1.91	
MC-REF20-01	4.38(*)	4.96	4.37	2.95
MC-REF20-02	5.55(**)		6.00	
MC-REF80-03	25.73	25.73	2.25	3.14
MC-REF80-04	34.56	40.34	3.65	5.18
MC-REF80-04a	46.12		3.14	

(*) F_{max} = 17.51kN multiplying by 4 (GFRP with 1/4 of the wide of other specimens).

(**) F_{max} = 22.19kN multiplying by 4 (GFRP with 1/4 of the wide of other specimens).

Preliminary considerations

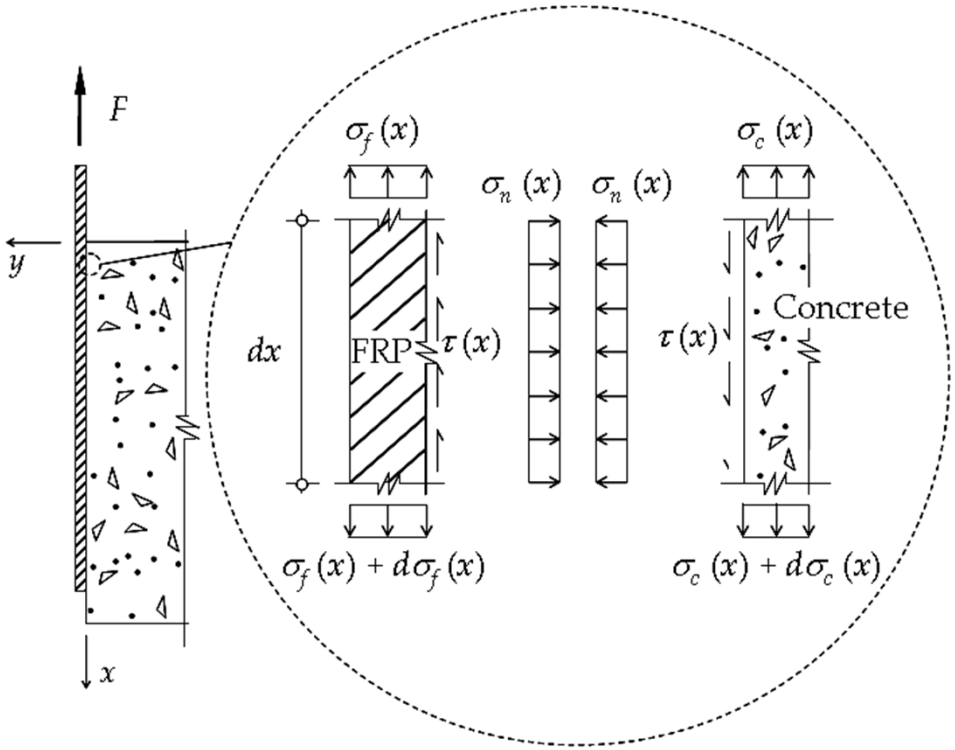

Calculating maximum bond stress…

From equilibrium and compatibility conditions of a finite element of FRP with length *dx*, it is obtained:

$$\frac{d^2 s}{dx^2} - \frac{\tau(s)}{E_f \cdot t_f} = 0$$

where *s* is the slip between FRP and concrete, $\tau(s)$ is the local bond stress, *x* is the coordinate axis along the bonded length, E_f and t_f, respectively, the Young modulus and the thickness of the FRP.

Assumptions:

i) $\varepsilon_f = ds/dx$, and ε_f is the FRP strain;

ii) linear and elastic behaviour is assumed for GFRP;

iii) bond is associated only with shear stresses, i.e., the normal stresses, σ_n, shown in figure above are considered of no influence.

Preliminary considerations

Calculating maximum bond stress…

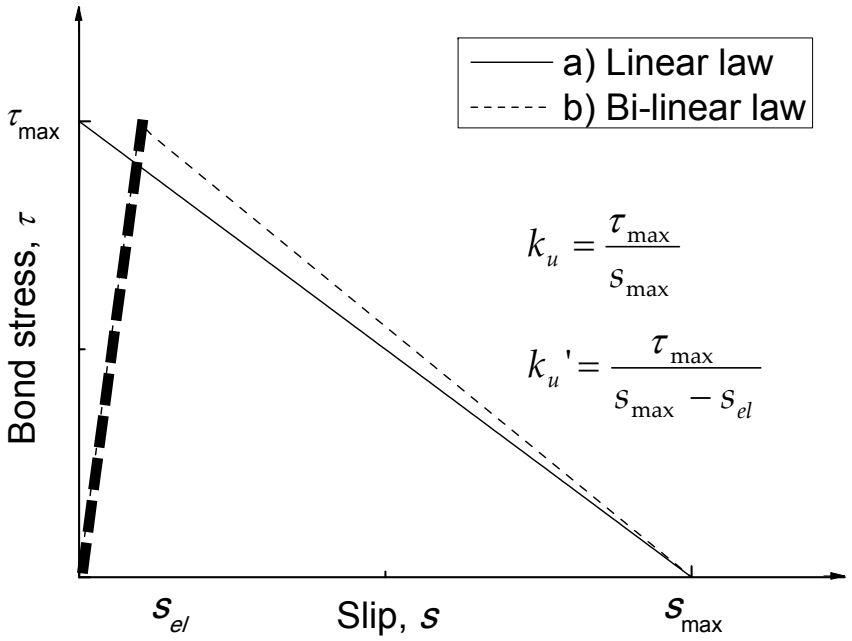

Assuming, for instance, the ascending branch of the bilinear bond-slip law and introducing the boundary conditions of the problem:

$$\frac{ds}{dx} = -\frac{F}{E_f \cdot A_f} \quad \text{at } x = 0$$

$$\frac{ds}{dx} = 0 \quad \text{at } x = L_{eff}$$

where A_f is the transversal area of the GFRP and L_{eff} is the effective bond length, the solution is given by:

$$s(x) = \frac{F}{\alpha \cdot E_f \cdot b_f \cdot t_f} \cdot \frac{\cosh(\alpha \cdot x - \alpha \cdot L_{eff})}{\sinh(\alpha \cdot L_{eff})}$$

$$\tau(x) = \frac{F \cdot \alpha}{b_f} \cdot \frac{\cosh(\alpha \cdot x - \alpha \cdot L_{eff})}{\sinh(\alpha \cdot L_{eff})} \Rightarrow \boxed{\frac{\tau_{max}(x=0)}{\tau_{avg}} = \frac{\pi}{2} \cdot \kappa \cdot \coth\left(\frac{\pi}{2} \cdot \kappa\right)} \quad \text{and} \quad \kappa = \frac{L_b}{L_{eff}}$$

Preliminary considerations

Calculating maximum bond stress…

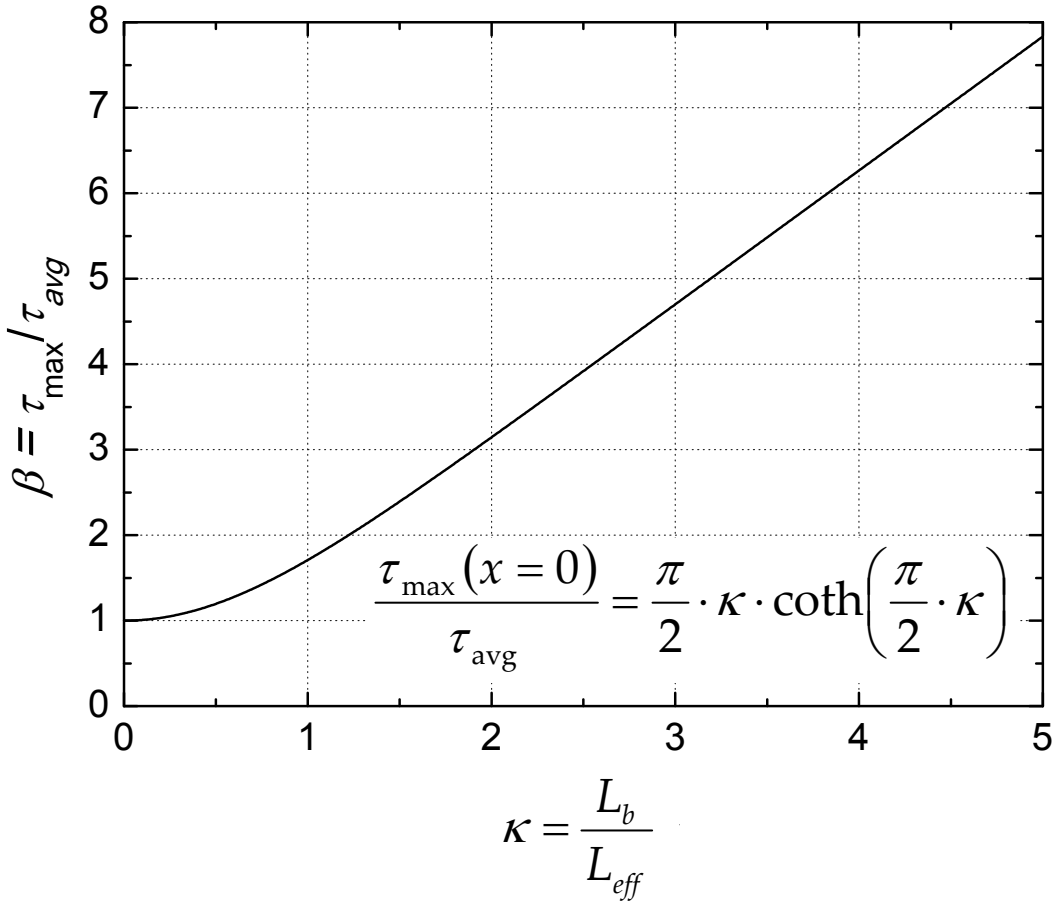

$$L_{eff} = \sqrt{\frac{E_f \cdot t_f}{c_2 \cdot f_{ctm}}}$$

Equation proposed by *fib* Bulletin 14 where c_2 = 2.0 in the case of CFRP.
In the case of GFRP, previous work, led to c_2 = 0.8.

Preliminary considerations

Comparing the maximum bond stress expected with some experimental works…

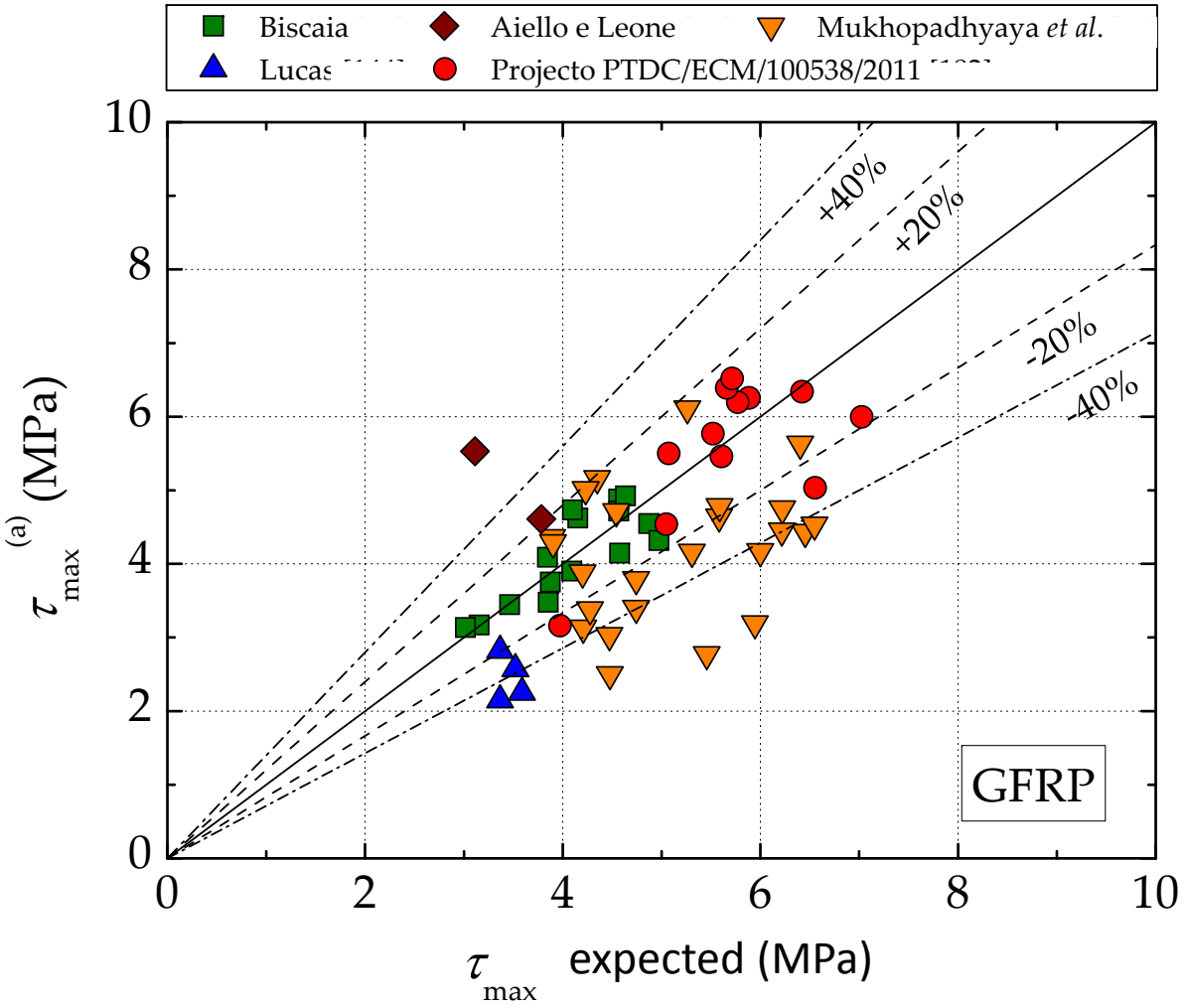

Experimental results

Reference specimens	Lateral compression stress, σ_L (MPa)	$\kappa = \frac{L_b}{L_{eff}}$	$\beta = \frac{\tau_{\max}}{\tau_{avg}}$	τ_{med} (MPa)	$\tau_{\max}$ (MPa)
MC-REF80-01	0.0	0.691	1.296	1.52	1.97
MC-REF80-02	0.0	0.682	1.288	1.40	1.81
MC-REF80-02a	0.0	0.682	1.288	1.21	1.56
MC-REF20-01	0.0	0.706	1.309	1.46	1.91
MC-REF20-02	0.0	0.706	1.309	1.85	2.42
MC-REF80-03	0.5	0.687	1.292	2.20	2.85
MC-REF80-04	1.0	0.699	1.303	2.91	3.79
MC-REF80-04a	1.0	0.689	1.294	3.94	5.09

1.78MPa

$\approx 1.6 \times \tau_{\max}^{0.0\text{MPa}}$

2.85MPa

4.44MPa

$\approx 2.5 \times \tau_{\max}^{0.0\text{MPa}}$

Experimental results

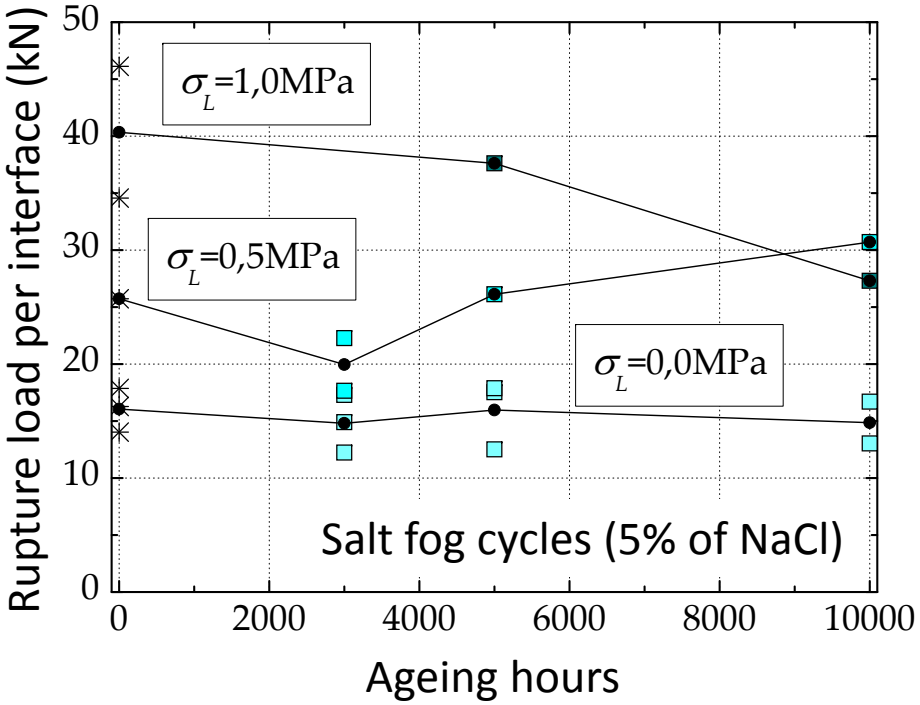

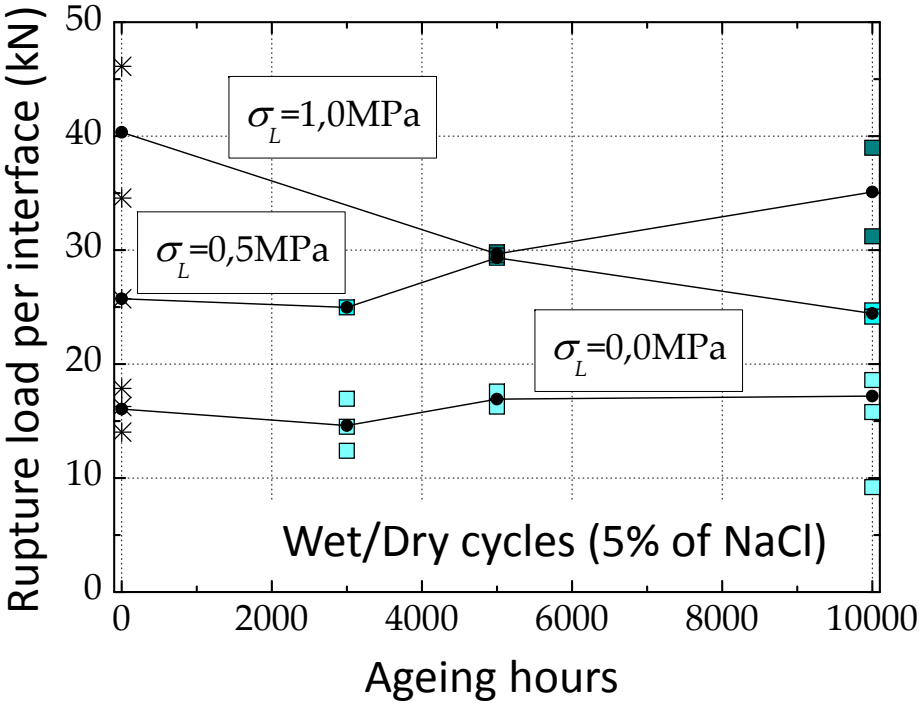

For σ_L = 1.0MPa a 35.0% of degradation was registered after 10,000h of exposure. However, improvement of the rupture load in the specimens with σ_L = 0.5MPa was registered after 10,000h of exposure.

For σ_L = 1.0MPa a 12.5% of degradation was registered after 10,000h of exposure. In the others situations there was no significant variations after 10,000h of exposure.

Experimental results

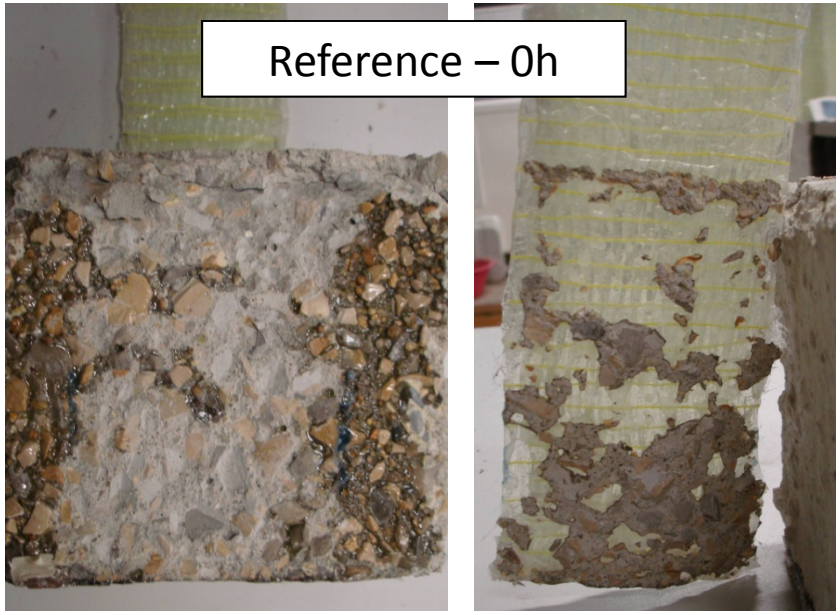

Cohesive rupture in the concrete!

The rupture surfaces of the specimens showed that the rupture mode changed from cohesive type by the concrete layer adjacent to the interface into adhesive type by the interface between both elements.

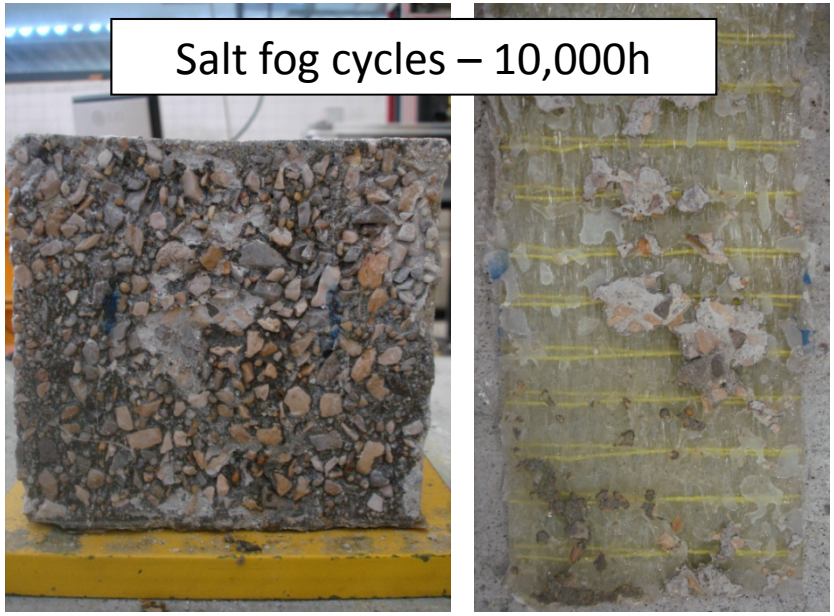

Adhesive rupture!

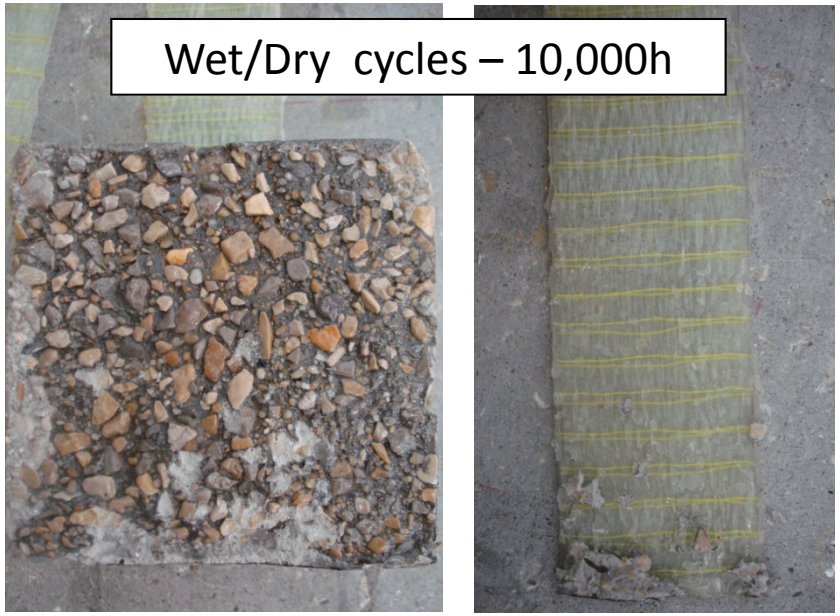

Adhesive rupture!

Rupture law

In order to study the GFRP/concrete interface and to establish a failure criterion based on the Mohr-Coulomb criterion, a research program is under development at Universidade Nova de Lisboa (UNL), based on double shear tests to obtain cohesion, *c*, and friction angle, ϕ. The figure below shows a typical envelope failure law (dotted line) defined according to equation:

$$\tau_{21} = c + \sigma_2 \times \tan\phi$$

where σ_2 is the confinement or lateral stress and τ_{21} is the shear stress.

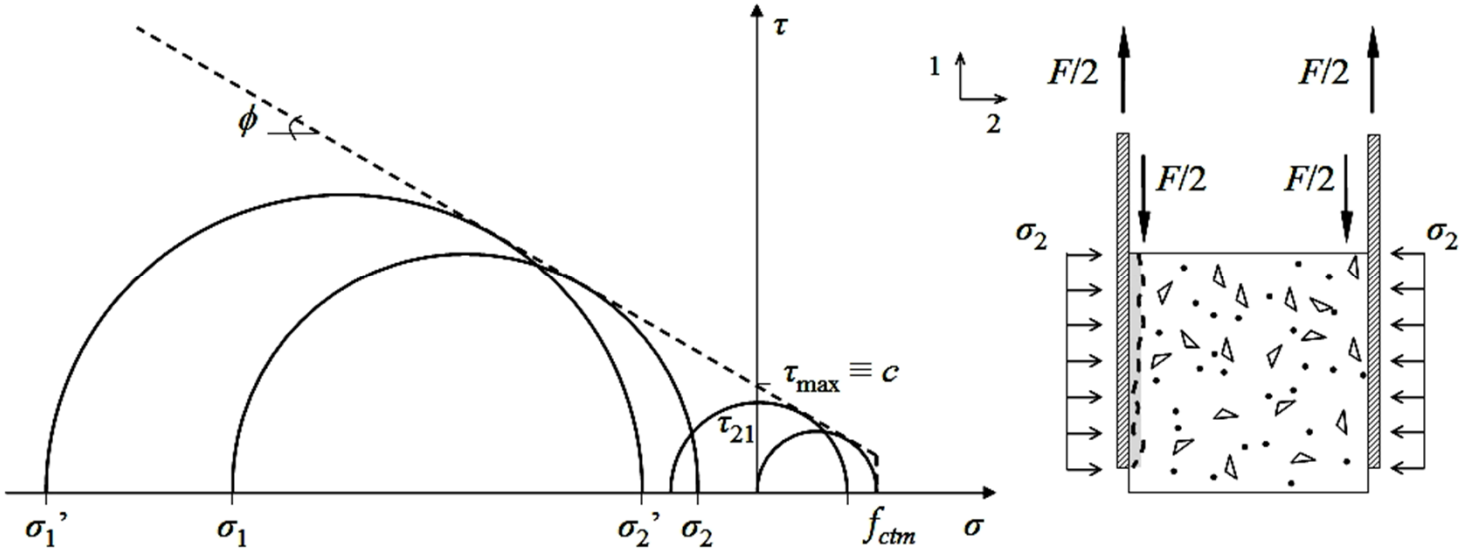

Specimens	Hours of ageing	Cohesion, *c* (MPa)	
MC-REF80-01	0	1,97	Losses/ Gains
MC-REF80-02	0	1,81	
MC-REF80-02a	0	1,56	
Average value	0	**1,78**	-
MC-NS-01	3000	1,36	-23,60%
MC-NS-01a	3000	1,93	8,43%
MC-NS-02	3000	1,64	-7,87%
MC-NS-04	5000	1,41	-20,79%
MC-NS-04a	5000	2,01	12,88%
MC-NS-05	5000	1,99	11,80%
MC-NS-08	10000	1,91	7,30%
MC-NS-09	10000	1,47	-17,42%
MC-MAR-01	3000	1,65	-7,30%
MC-MAR-02	3000	1,43	-19,66%
MC-MAR-02a	3000	1,97	10,67%
MC-MAR-04	5000	1,99	11,80%
MC-MAR-05	5000	1,82	2,25%
MC-MAR-08	**10000**	**1,07**	**-39,89%**
MC-MAR-08a	10000	2,16	21,35%
MC-MAR-09	10000	1,85	3,93%

Rupture law

In terms of mean value, at 10,000h, the salt fog cycles revealed a degradation of 5.1%.

However, for wet/dry cycles, ignoring the value obtained from the MC-MAR-08 (1,07MPa), at 10,000h of exposure, cohesion increase almost 13%.

Note also that the variation of cohesion corresponds to the variation of the maximum bond stress in the specimens without lateral compression stress.

Rupture law

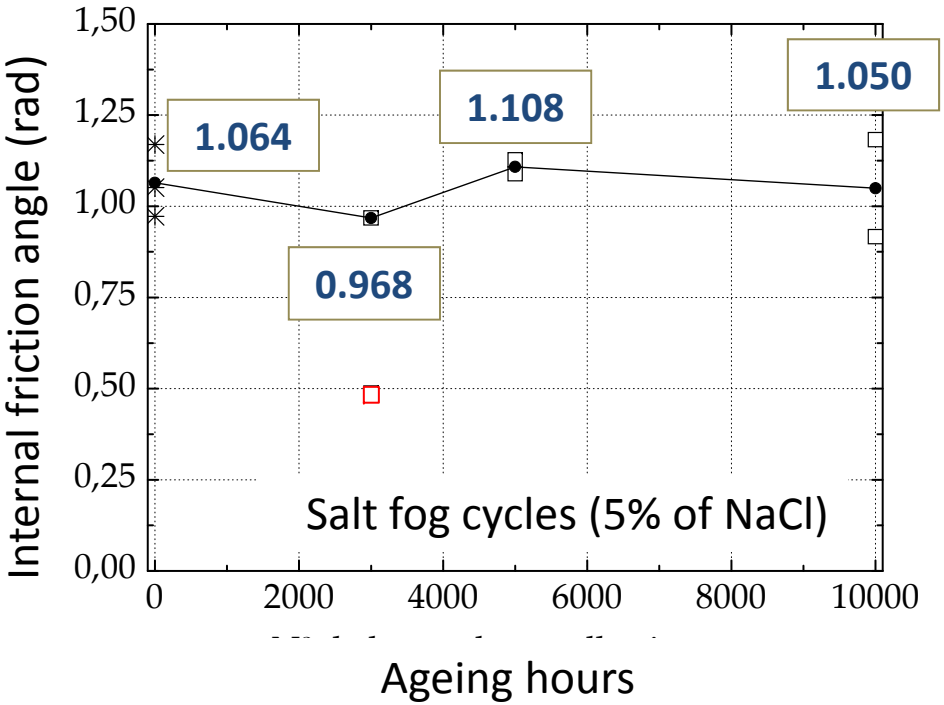

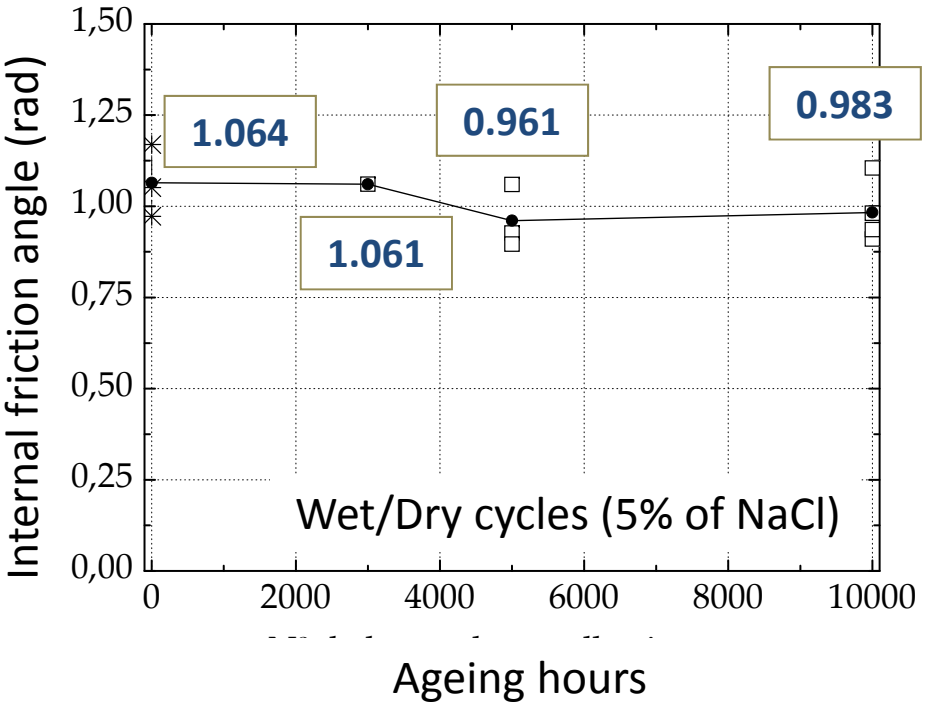

Internal friction angle did not varied significantly. The greater variation was calculated at 5,000h hour of exposure. However, at that time only one specimen was considered.
With 10,000h of exposure, the internal friction angle of the GFRP/concrete interface reduced only 1.3%.

After 5,000h of exposure, internal friction angle decreased approximately 10%.

Modeling with FE

So far, only the reference specimens were modulated with FE...

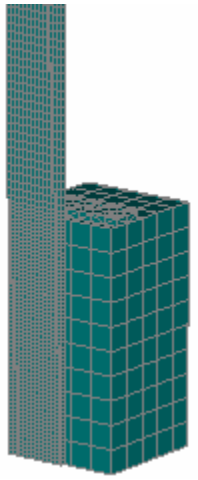

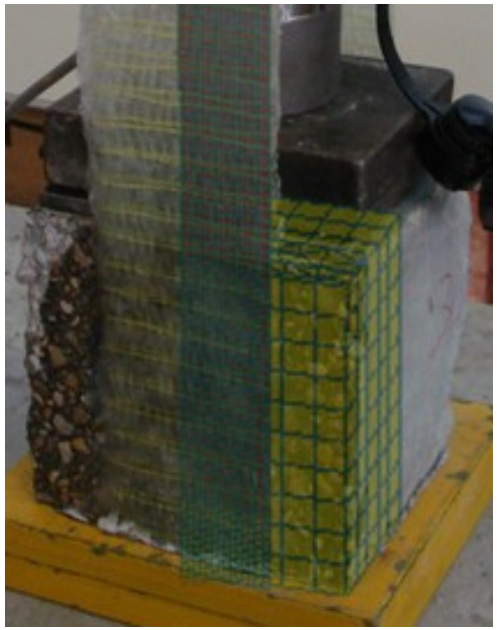

The concrete element discretization was done with quadrilateral elements with 15mm and, to precisely investigate the interfacial behaviour of the GFRP/concrete interface, the solid brick elements used to represent GFRP had 2.5mm near to the contact with concrete. A coarse mesh of 5.0mm was adopted for the GFRP element more distant from the contact. Compatibly mesh in the GFRP element was always guaranteed.

In order to avoid a model with a high number of FE, a quarter of the specimens were also considered based on the symmetric conditions of the tests. In total, 2411 3D elements were used corresponding to a total of 4956 nodes. In the figure it is visible the standard model with the respectively mesh used in this work.

Modeling with FE

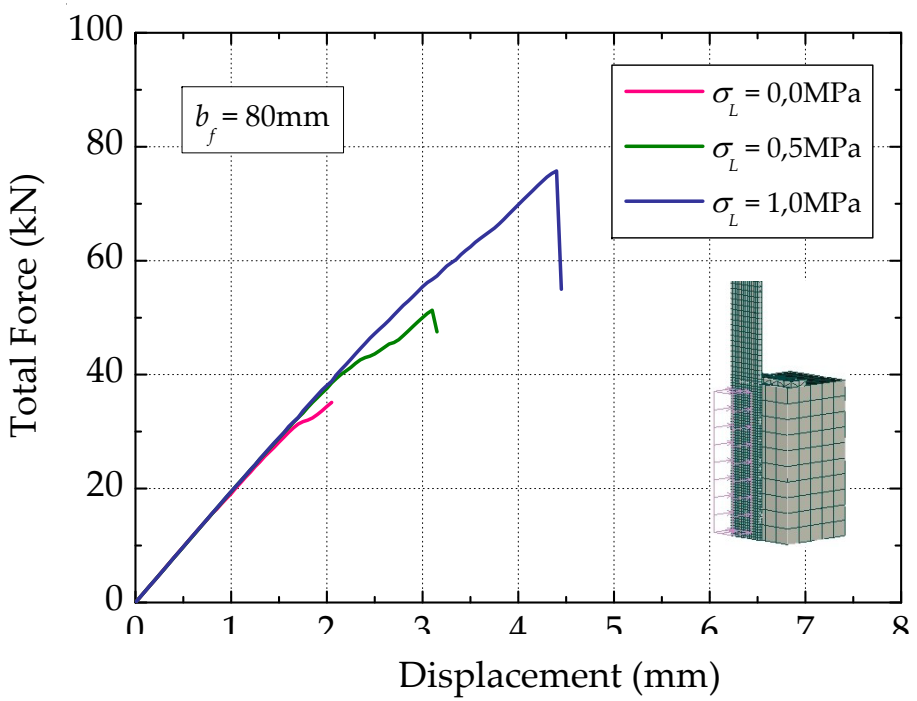

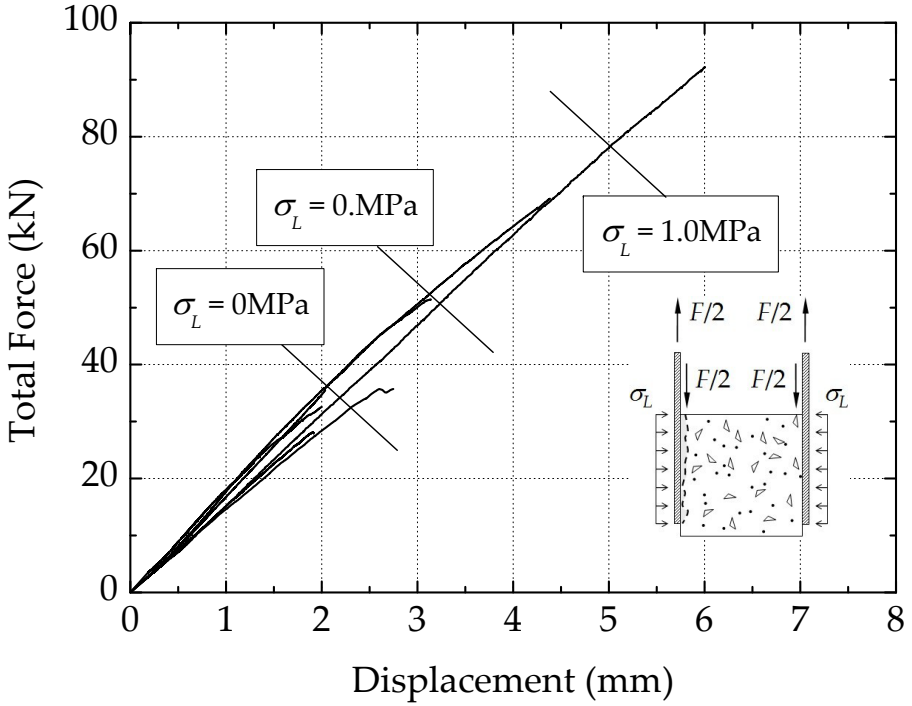

Specimen	σ_L (MPa)	F_{max} (kN)		Error (%)	δ_{max} (mm)		Error (%)
		Exp. (*)	ATENA 3D		Exp. (*)	ATENA 3D	
MC-REF80	0,0	16,06	17,57	9,40	2,20	2,05	-6,82
MC-REF80	0,5	25,73	25,66	-0,27	3,14	3,10	-1,27
MC-REF80	1,0	40,34	37,88	-6,10	5,18	4,40	-15,06

(*) Average values obtained from the experimental tests.

Modeling with FE

Rigid interface

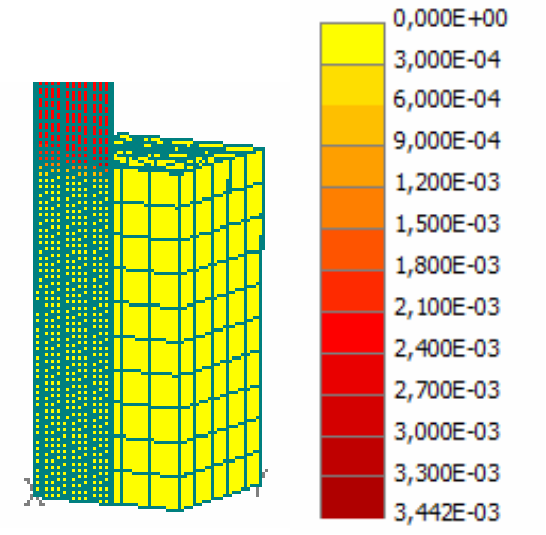

Gap interface

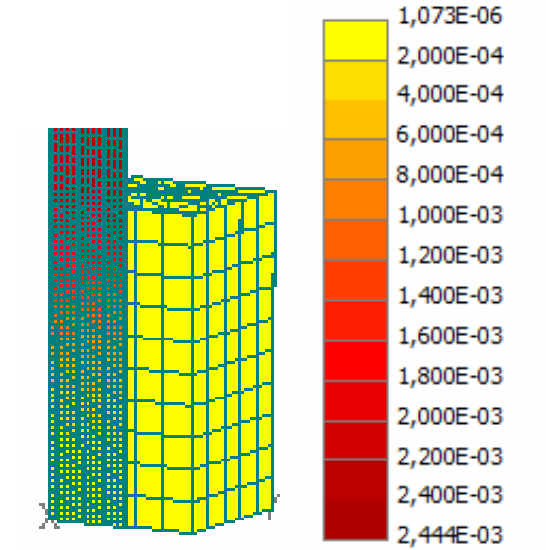

Principal maximum strains

Assuming a rigid GFRP/concrete interface is a somewhat crude manner of modelling an EBR concrete structure. Phenomena like slip, displacements between FRP and concrete, or normal and bond stress distribution along the interface are neglected. Moreover, the rupture mode and even the rupture instant are only controlled by the experimental values of the ultimate strengths of all materials involved in the test. Nevertheless, the load *versus* displacements behaviour is quite stiffer when compared with the experimental or with the gap interface FE. The stress distribution along the GFRP is completely different when compared to the gap interface FE and, as explained above, the rupture mode occurs for the ultimate strain of the GFRP, i.e., for 2.20%. Hence, the rigid interface model cannot predict the rupture mode.

Modeling with FE

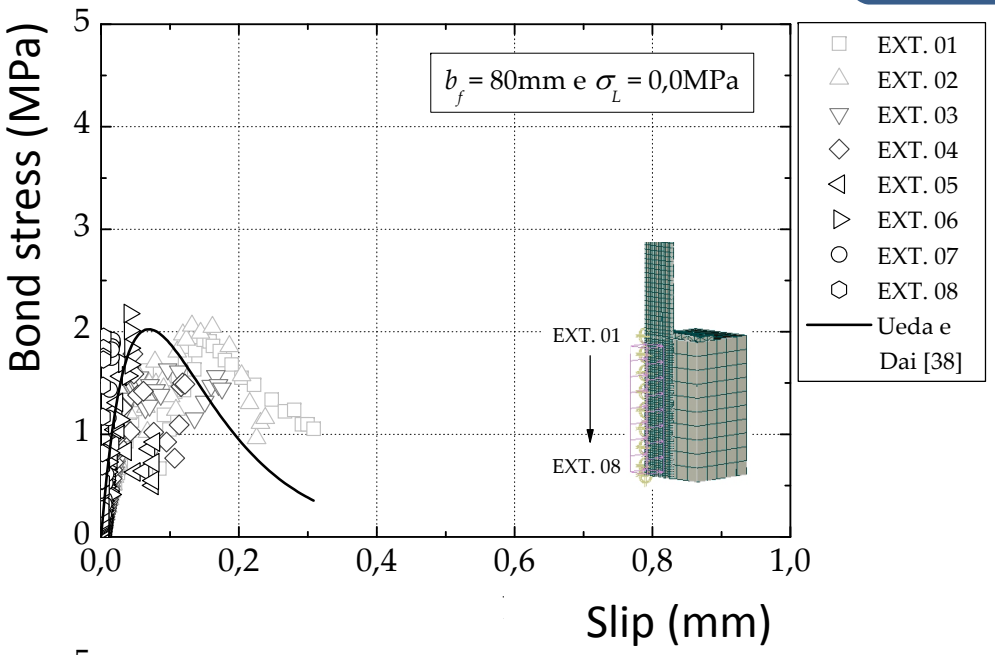

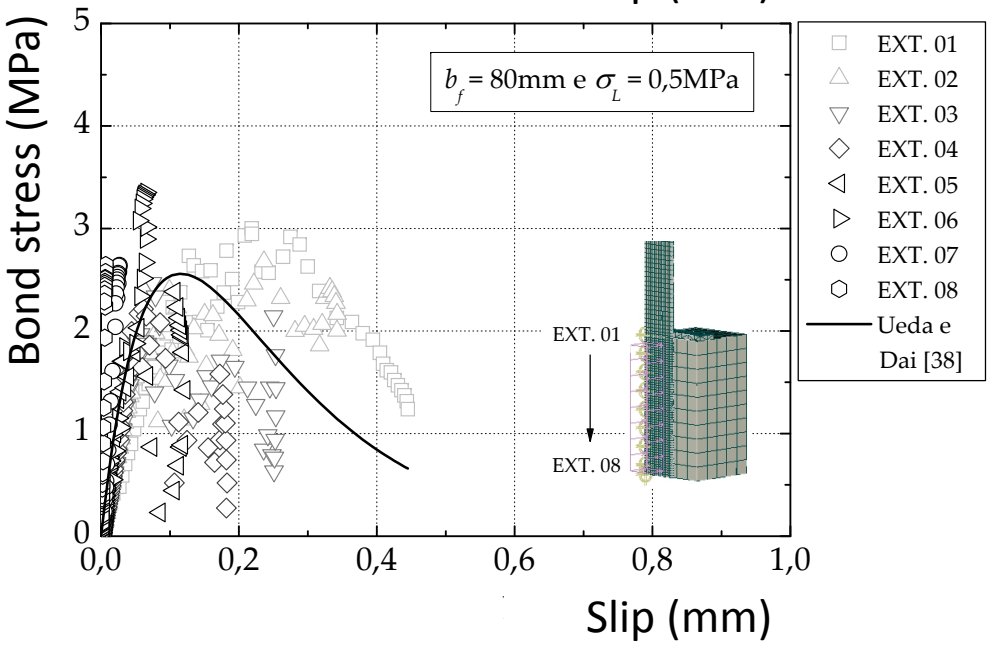

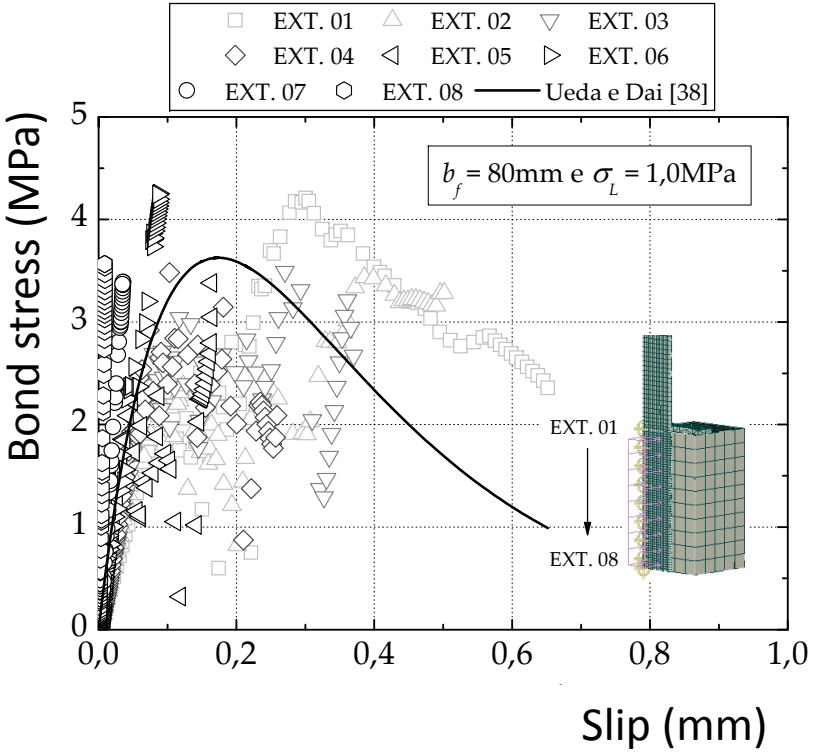

Results obtained by Ueda and Dai methodology.

Modeling with FE

The principal strains in GFRP and concrete weren't reached at any step of the FEA and thus, the collapse of the shear tests weren't by rupture of these elements. This evidence leads to another, and unique, possible failure mode which is the debonding of the GFRP and concrete. Hence, the FEA also predicted with fairly agreement the rupture mode. The debonding phenomenon is quite visible in the model as shown in figure and it is in total accordance with the failure obtained in the experiments.

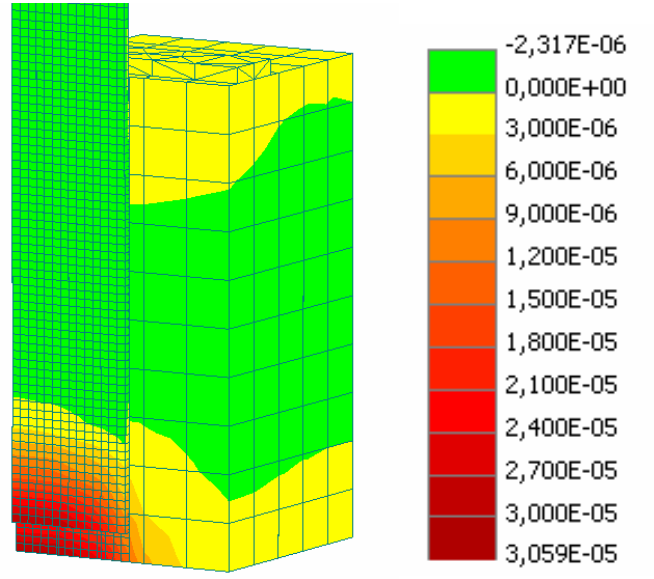

FE detail of the GFRP/concrete interface at maximum load (MC1-FEA model - vertical displacements amplified 10 times).

Modeling with FE

FE results at maximum load instant.

b_f = 80mm e σ_L = 0,0MPa

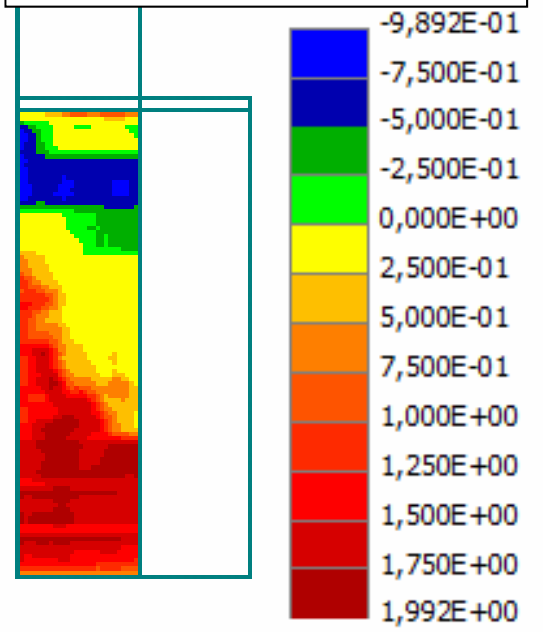

b_f = 80mm e σ_L = 0,5MPa

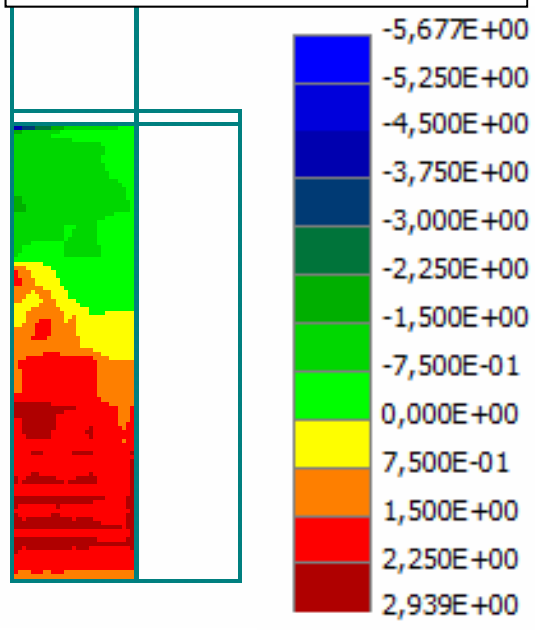

b_f = 80mm e σ_L = 1,0MPa

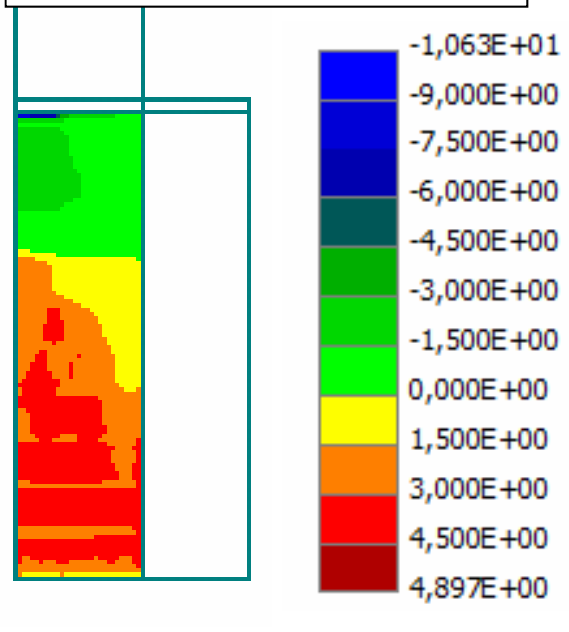

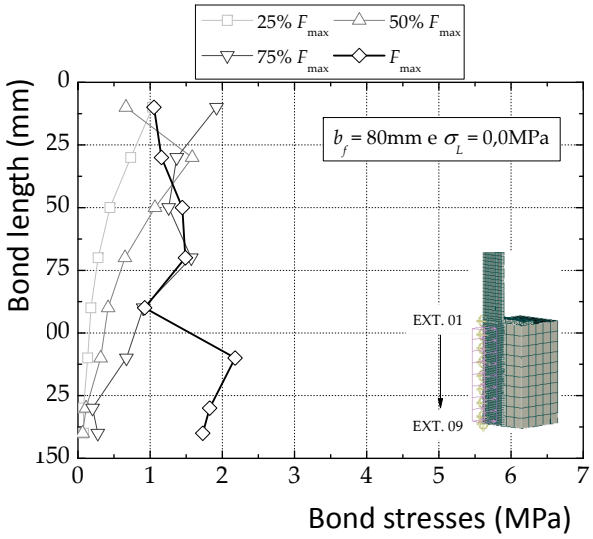

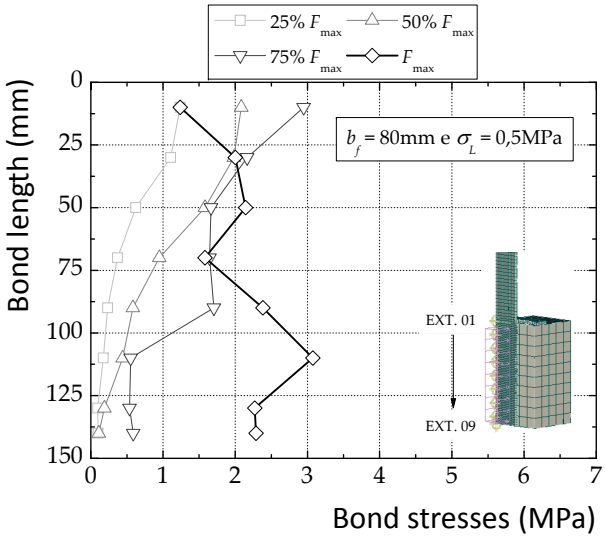

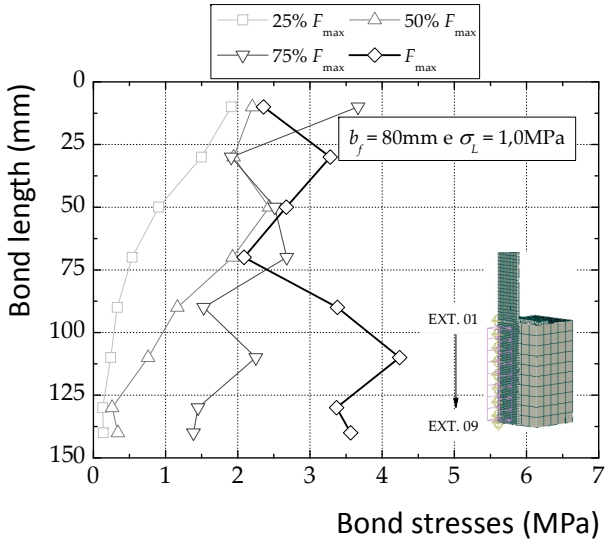

Modeling with FE

Applicable fields:

Externally Bonded Reinforcement (EBR) of Beams:

EBR of Slabs:

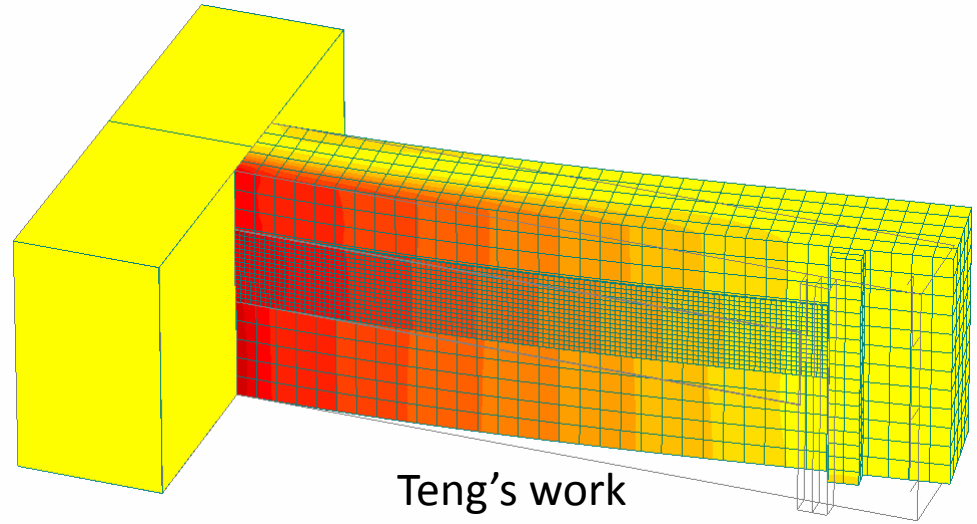

Teng's work

Conclusions

Main conclusions are:

1. The shear tests permitted to define parameters like cohesion and friction angle of the GFRP/concrete interface;
2. The proposed tests and obtained results may permit the estimation and quantification of different failure laws for different concrete classes and for different environmental ageing tests;
3. The rupture modes of the reference specimens were all essentially cohesive and in concrete;
4. The number of the ageing hours lead to a change of the failure mode from cohesive type to adhesive type. However, the specimens with a lateral compression stress involved some peeling that led to an increase of that stress for higher loads, i.e., at instants closed to the specimen failure;
5. The results are the support for the definition of a failure envelope law that can be applied to FE of an interface based on the Mohr-Coulomb failure criterion. Some preliminary results already showed a good accuracy and more efforts are now being done in order to improve the understanding of the influence of the surface treatment and the environmental ageing in those failure laws;
6. The interface FE may be applied in different concrete structures externally reinforced with GFRP.

THANK YOU

The authors are grateful to Fundação para a Ciência e Tecnologia for partial financing of the work under Project PTDC/ECM/100538/2008. The authors would like to thank for the help of Prof. Vladimir Cervenka and Ing. Dobromil Pryl, with ATENA.

FACULDADE DE CIÊNCIAS E TECNOLOGIA
UNIVERSIDADE NOVA DE LISBOA